SHED-derived exosomes ameliorate hyposalivation caused by Sjögren's syndrome via Akt/GSK-3β/Slug-mediated ZO-1 expression

Zhihao Du[1], Pan Wei[2], Nan Jiang[3], Liling Wu[4], Chong Ding[3], Guangyan Yu[1]

[1]Department of Oral and Maxillofacial Surgery, Peking University School and Hospital of Stomatology & National Center of Stomatology & National Clinical Research Center for Oral Diseases & National Engineering Research Center of Oral Biomaterials and Digital Medical Devices, Beijing 100081, China;
[2]Department of Oral Medicine, Peking University School and Hospital of Stomatology & National Center of Stomatology & National Clinical Research Center for Oral Diseases & National Engineering Research Center of Oral Biomaterials and Digital Medical Devices, Beijing 100081, China;
[3]Center Laboratory, Peking University School and Hospital of Stomatology & National Center of Stomatology & National Clinical Research Center for Oral Diseases & National Engineering Research Center of Oral Biomaterials and Digital Medical Devices, Beijing 100081, China;
[4]Department of Physiology and Pathophysiology, Peking University School of Basic Medical Sciences, Key Laboratory of Molecular Cardiovascular Sciences, Ministry of Education, and Beijing Key Laboratory of Cardiovascular Receptors Research, Beijing 100191, China.

Abstract

Background: Sjögren's syndrome (SS) is an autoimmune disorder characterized by sicca syndrome and/or systemic manifestations. The treatment is still challenging. This study aimed to explore the therapeutic role and mechanism of exosomes obtained from the supernatant of stem cells derived from human exfoliated deciduous teeth (SHED-exos) in sialadenitis caused by SS.

Methods: SHED-exos were administered to the submandibular glands (SMGs) of 14-week-old non-obese diabetic (NOD) mice, an animal model of the clinical phase of SS, by local injection or intraductal infusion. The saliva flow rate was measured after pilocarpine intraperitoneal injection in 21-week-old NOD mice. Protein expression was examined by western blot analysis. Exosomal microRNA (miRNAs) were identified by microarray analysis. Paracellular permeability was evaluated by transepithelial electrical resistance measurement.

Results: SHED-exos were injected into the SMG of NOD mice and increased saliva secretion. The injected SHED-exos were taken up by glandular epithelial cells, and further increased paracellular permeability mediated by zonula occluden-1 (ZO-1). A total of 180 exosomal miRNAs were identified from SHED-exos, and Kyoto Encyclopedia of Genes and Genomes analysis suggested that the phosphatidylinositol 3 kinase (PI3K)/protein kinase B (Akt) pathway might play an important role. SHED-exos treatment down-regulated phospho-Akt (p-Akt)/Akt, phospho-glycogen synthase kinase 3β (p-GSK-3β)/GSK-3β, and Slug expressions and up-regulated ZO-1 expression in SMGs and SMG-C6 cells. Both the increased ZO-1 expression and paracellular permeability induced by SHED-exos were abolished by insulin-like growth factor 1, a PI3K agonist. Slug bound to the ZO-1 promoter and suppressed its expression. For safer and more effective clinical application, SHED-exos were intraductally infused into the SMGs of NOD mice, and saliva secretion was increased and accompanied by decreased levels of p-Akt/Akt, p-GSK-3β/GSK-3β, and Slug and increased ZO-1 expression.

Conclusion: Local application of SHED-exos in SMGs can ameliorate Sjögren syndrome-induced hyposalivation by increasing the paracellular permeability of glandular epithelial cells through Akt/GSK-3β/Slug pathway-mediated ZO-1 expression.

Keywords: Stem cells from human exfoliated deciduous teeth; Exosomes; Saliva; Sjögren's syndrome; Submandibular gland

Introduction

Sjögren's syndrome (SS) is a systemic autoimmune disease histopathologically characterized by lymphocytic infiltration of exocrine glands such as the salivary and lacrimal glands, leading to destruction and dysfunction present with sicca symptoms (dry mouth and dry eye).[1,2] According to the literature, >95% of SS patients present with sicca symptoms, 70% of patients have systemic symptoms such as fatigue and musculoskeletal pain. Glandular dysfunction has a chronic course and might remain stable for a long period of time (up to 12 years).[3] In addition, approximately 60% of SS patients coexist with other autoimmune diseases, such as rheumatoid arthritis and autoimmune thyroid disease.[4] Mucocutaneous manifestations are also commonly seen in SS patients.[5] These all have an important impact on health-related quality of life and even worse, threaten life.

Access this article online

Quick Response Code:

Website: www.cmj.org

DOI: 10.1097/CM9.0000000000002610

Correspondence to: Guangyan Yu, Department of Oral and Maxillofacial Surgery, Peking University School and Hospital of Stomatology, No. 22, Zhongguancun South Avenue, Haidian District, Beijing 100081, China
E-Mail: gyyu@263.net;
Chong Ding, Center Laboratory, Peking University School and Hospital of Stomatology, No. 22, Zhongguancun South Avenue, Haidian District, Beijing 100081, China
E-Mail: idtbbsb@163.com

Chinese Medical Journal 2023;136(21)
Received: 31-12-2022; **Online:** 12-04-2023 **Edited by:** Lishao Guo

As a systemic autoimmune disease, the treatment of SS is still challenging. Traditional therapeutic schedules are focused on relieving SS with artificial tears and saliva and even inducing their production.[6] Others are concentrated on suppressing the immune system with immunosuppressant and immunomodulatory drugs.[7,8] However, the former cannot repair the damaged glands and restore their function,[6] and the long-term use of immunosuppressant drugs might increase the risk of infection and the incidence of metabolic disorders and result in cardiovascular disease.[7,9] Recently, intravenous injection of bone marrow mesenchymal stem cells (BMMSCs), umbilical cord mesenchymal stem cells, and conditioned media from dental pulp stem cells have been reported to alleviate the decreased saliva secretion in experimental and clinical SS.[10,11] Nevertheless, implanted mesenchymal stem cells (MSCs) will not survive for a long time *in vivo*, and the injected cells cannot migrate to the damaged glands.[12,13] Moreover, the conditioned media contains numerous and diverse cytokines, and defining the exact factors that work is complex.[11,14-16] Therefore, it is critical to determine an effective strategy that is easy to produce with stable performance and clear composition.

Exosomes, as described as mini-maps of their cells of origin, are extracellular microvesicles with a diameter range of 30 to 150 nm that are positive for cluster of differentiation 63 (CD63) and heat shock protein 70 (HSP70).[17,18] Compared with stem cells, exosomes have shown more potential advantages for clinical application, including (but not limited to) an absence of need for systemic administration and no self-replication.[19] Recently, exosomes have attracted increasing attention in cell therapy. For example, the antitumor activities of MSCs are largely mediated through exosome-established multidirectional communication in the tumor microenvironment.[20] BMMSC-derived exosomes are found to induce long-term neuroprotection and promote neuroregeneration and neurological recovery in a rodent stroke model at the same time.[21,22] Stem cell-derived exosomes improve ischemia/reperfusion injury in rat lungs.[23] Stem cells from human exfoliated deciduous teeth (SHEDs) have been isolated and named by Miura *et al*[24] in 2003 for the first time. Our recent study has shown that intravenous injection of SHEDs protects gland function, avoiding immune damage, in 7-week-old non-obese diabetic (NOD) mice, which represents an initial phase of SS.[12] However, with respect to patients in the clinical phase of SS displaying developed inflammation and gland dysfunction, it needs to be elucidated whether SHED-derived exosomes (SHED-exos) have a therapeutic effect on sialadenitis, as well as the underlying mechanism of this effect.

Therefore, the purposes of the present study were to explore the therapeutic effects of SHED-exos on the structure and functional injury caused by SS and to further reveal the underlying mechanism of increasing saliva secretion of the damaged glands by SHED-exos.

Methods

Ethical approval

The study was approved by the Institutional Review Board of Peking University School of Stomatology (No. PKUSSIRB-201950162). Participants were informed about the research project, and informed consent forms were signed. Mice were used under the ethical approval and the ethical guidelines of the Peking University Institutional Review Board (No. LA2019109).

Cell and tissue culture

SHEDs were provided by the ORAL STEM CELL BANK (Beijing Tason Biotech Co., Beijing, China) and cultured in MSC medium containing 10% fetal bovine serum (FBS), 100 μg/mL streptomycin, and 100 U/mL penicillin. Human immortalized keratinocytes (HaCaTs) were purchased from American Type Culture Collection (Rockville, MD, USA) and cultured in Dulbecco's modified Eagle's medium (DMEM) containing 10% FBS, 100 μg/mL streptomycin, and 100 U/mL penicillin. Human submandibular gland (SMG) tissues were obtained from five patients (45–58 years old; three females) who had primary oral squamous cell carcinoma but had not received irradiation and chemotherapy and were undergoing functional neck dissection as part of surgical treatment. All the collected tissues were histologically confirmed as normal. For acinar cell preparation, the gland tissue was minced on ice and digested with collagenase (Worthington, Lakewood, USA) and 1% bovine serum albumin (BSA) for 60 min as reported previously.[25] Duct cells were cultured from Wharton's duct tissues with high expression of creatine kinase 8 (CK8) and low expression of α-amylase. For tissue culture, the fresh gland tissues were minced into small pieces (0.5 mm^3) and cultured with or without SHED-exos for 24 h at 37°C. Damaged labial gland samples were obtained from four SS patients (25–45 years old; three females, diagnosis according to the American College of Rheumatology/European League Against Rheumatism Criteria) in Peking University School of Stomatology, and the labial glands obtained from four mucocele patients served as normal controls. The fresh gland tissues were minced into small pieces (0.5 mm^3) and cultured with or without SHED-exos for 24 h at 37°C. The SMGs of 14-week-old NOD mice were collected. The fresh gland tissues were minced into small pieces and cultured with or without SHED-exos for 24 h at 37°C. Then, all the cultured tissues were collected for further examination. The rat submandibular epithelial cell line with characteristics of acinar cells (SMG-C6, a generous gift from Dr. David O. Quissell) was routinely cultured in DMEM/F12 (1:1 mixture) containing 5 μg/mL transferrin, 2 nmol/L triiodothyronine, 1.1 μmol/L hydrocortisone, 0.1 μmol/L retinoic acid, 5 mmol/L glutamine, 80 ng/mL epidermal growth factor, 50 μg/mL gentamicin sulfate, 5 μg/mL insulin, 100 U/mL penicillin, 100 μg/mL streptomycin, and 2.5% FBS.[26] All cell and tissue culture constituents were purchased from Gibco (Rockville, USA) and Sigma-Aldrich (St Louis, USA).

Exosome isolation and identification

Exosomes were collected from the supernatants of SHEDs and HaCaTs (both cultured in exosome-free medium with exosome depleted FBS) and isolated by ultracentrifugation and sucrose cushion as described previously.[27] For identification, SHED-exos were stained with

phosphotungstic acid and examined with a transmission electron microscope (JEM-1400 electron microscope, JOEL, Japan). Furthermore, the size distribution and particle concentration were determined by nanoparticle tracking analysis with a NanoSight NS300 (Malvern, UK) and 3.2 DevBuild 3.2.16.

SHED-exos treatment

The 7- and 14-week-old female NOD mice and age-matched BALB/c mice used in the study were obtained from Peking University Health Science Center. The investigation conformed to the Guide for the Care and Use of Laboratory Animals published by the US National Institutes of Health. All animal surgeries were performed under anesthesia, and all efforts were made to minimize suffering. For injection, 50 μg SHED-exos (diluted in 25 μL phosphate buffer saline [PBS]) were injected into the SMGs at multiple points in 14-week-old NOD mice, which represents the clinical phase of SS. For intraductal infusion, the intraoral duct orifice of the SMG was inserted with an intrathecal catheter system (11.7 cm, 32 g accepts, 27 g needles) and perfused with 50 μg SHED-exos into 14-week-old NOD mice. Equal volume of PBS was perfused as control and 50 μg HaCaT-exos (diluted in 25 μL PBS) was injected as the "sham" exos. The mice were euthanized after 21 weeks, and the SMGs were collected.

Stimulated saliva flow rate measurement

Under anesthesia, the mice were intraperitoneally injected with pilocarpine (0.05 mg/100 g body weight), and then the whole saliva was collected with a micropipette from the oral cavity for 10 min. The weight of the saliva was measured with a precision weighing balance (METTLER TOLEDO, Columbus, USA).

Hematoxylin-eosin staining and histological evaluation

The SMG tissues of mice were surgically removed and fixed with 4% paraformaldehyde and embedded in paraffin wax. The specimens were serially cut into 5 μm thick sections and stained with hematoxylin and eosin. The sections were observed under a microscope for lymphocytic infiltration. The degree of inflammation was assessed and averaged from three different randomly selected fields in each sample from six SMGs of each group. The focus score was defined as the number of foci comprising ≥50 mononuclear cells per 4 mm^2 of gland tissue and the ratio index was defined as the ratio of the foci area to the tissue total area.

SHED-exos labeling and tracking

SHED-exos were incubated with 1,1-dioctadecyl-3,3,3,3-tetramethylindotricarbocyanine iodide (DiR; Invitrogen, Carlsbad, Calif, USA) and PKH26 (Sigma-Aldrich) and then injected into the glands. The bioluminescence was measured using the *in vivo* Imaging Systems (IVIS) (Caliper Life Sciences, Hopkinton, USA). Next, PKH26-labeled SHED-exos were incubated with SMG-C6 cells, primary cultured human SMG acinar cells, and duct cells for 24 h. The above images were captured by confocal microscopy (LMS710, Carl Zeiss Microscopy, Oberkochen, Germany).

Real-time polymerase chain reaction (PCR)

Total RNA from four control and four SS labial gland tissues was extracted using TRIzol reagent (Invitrogen), and copy DNA (cDNA) was synthesized using a cDNA Reverse Transcription Kit (Takara, Tokyo, Japan). PCR was conducted with FastStart Universal SYBR Green Master reagent (Roche, Mannheim, Germany) as described on the ABI Prism 7500 real-time PCR system (Applied Biosystems, Waltham, USA). The total mRNA extracted from each sample was performed real-time PCR in triplicate and the primer sequences used are listed in Supplementary Table 1, http://links.lww.com/CM9/B445.

Microarray analysis

SHED-exos extracted from three individual SHEDs samples were analyzed with an Agilent Human miRNA microarray (v21.0; Agilent Technologies Inc., Santa Clara, USA). The original data files were processed by Feature Extraction software (Agilent Technologies, Inc.). Signals were normalized using Gene Spring GX software 11.0 (Agilent Technologies). The target genes of exosamal microRNA (miRNAs) underwent further Kyoto Encyclopedia of Genes and Genomes (KEGG) pathway classification analysis.

Western blotting analysis

SMG tissues and SMG-C6 cells were harvested in lysis buffer (RIPA buffer, #89900, Thermo Fisher Scientific, Waltham, USA) and ultrasonicated at 4°C for 30 s. After centrifugation at 12,000 ×*g* for 10 min, the protein concentrations were determined using a bicinchoninic acid protein assay kit (MPK002; M&C Gene Technology, Beijing, China). The proteins (30 μg) were separated by 12% sodium dodecyl sulfate polyacrylamide gel electrophoresis (SDS-PAGE), transferred to polyvinylidene fluoride membranes, probed with primary antibodies, and then incubated with horseradish peroxidase-conjugated secondary antibodies (ZSGB-BIO, Beijing, China). The target proteins were detected using enhanced chemiluminescence reagent (Huaxingbio, Beijing, China). Detailed information on the antibodies is listed in Supplementary Table 2, http://links.lww.com/CM9/B445. Immunoreactive band intensities were calculated with ImageJ software v1.8.0 (National Institutes of Health, Bethesda, USA).

Immunofuorescence staining

SMG-C6 cells cultured on glass coverslips were fixed in 4% paraformaldehyde and permeabilized with 0.1% Triton X-100. Once they were blocked with 1% BSA, cells were incubated with anti-zonula occluden-1 (ZO-1) and anti-occludin antibodies at 4°C overnight, and then incubated with Alexa Fluor 594- or Alexa Fluor 488-conjugated secondary antibodies. Nuclei were stained with 4′, 6-diamidino-2-phenylindole. Fluorescence images were captured by a laser scanning confocal microscope (TCS SP8, Leica, Wetzlar, Germany).

Transepithelial electrical resistance (TER) measurement

Confluent monolayers of SMG-C6 cells were grown in 24-well Transwell™ chambers (Corning Costar, Cambridge, USA) for 7 days, and then TER was measured at 37°C using an Epithelial Volt Ohm Meter (WPI, FL, USA). TER values were calculated by subtracting the blank filter (90 Ω) and by multiplying the surface area of the filter.

ZO-1 knockout and rescue

SMG-C6 cells were transfected with the ZO-1 small guide RNA (sgRNA) plasmid (sequence: TTCACCAATGT-GACCTTGGT; Genechem Inc., Shanghai, China). Scrambled guide RNA plasmids were used as a negative control. For re-expression ("rescue"), ZO-1 knockout SMG-C6 cells were cultured to 60% confluency and transfected with ZO-1 cDNA plasmids (#30313, Addgene, http://www.addgene.org).

Double luciferase reporter gene assay

A rat ZO-1 promoter fragment was amplified by PCR and inserted into the pGL3 vector. HEK293T cells were transfected with plasmids expressing the ZO-1 promoter region or Slug. For normalization, the Renilla luciferase reporter construct was cotransfected. All luciferase assays were analyzed after 24 h of transfection using a Dual-Luciferase Kit (Promega, Madison, USA) according to the manufacturer's protocol.

Statistical analysis

Data are shown as the mean ± standard deviation or mean ± standard error. Statistical analysis was performed by unpaired Student's *t*-test between two groups or one-way analysis of variance followed by Bonferroni's test among multiple groups using Prism 6.0 software (GraphPad, San Diego, USA). $P < 0.05$ was considered statistically significant.

Results

SHED-exos increase saliva secretion and ameliorate lymphocytic infiltration in the SMGs of NOD mice

SHED-exos extracted from SHEDs culture supernatant were identified and showed a standard microstructure [Figure 1A], and they expressed the exosome-associated proteins CD9, CD63, CD81, and HSP70 [Figure 1B]. The mean diameter of SHED-exos was 126.5 ± 5.7 nm [Figure 1C]. The stimulated saliva flow rate was significantly decreased in 14-week-old NOD mice and further dropped in 21-week-old NOD mice compared with 7-week-old NOD mice and age-matched BALB/c mice [Figure 1D]. To explore the therapeutic effect of SHED-exos on sialadenitis, we injected 50 μg SHED-exos into the SMGs of 14-week-old NOD mice and euthanized the mice at 21 weeks. SHED-exos significantly increased the stimulated saliva flow rate compared with those in age-matched untreated, PBS-treated, and HaCaT-exo-treated groups. Inflammatory cell infiltration in the SMGs is shown in Figure 1E and Supplementary Figure 1, http://links.lww.com/CM9/B445. Moreover, quantitative analysis showed that the focus score and the ratio index were increased in 21-week-old NOD mice, but both of them were significantly decreased in the SHED-exo-treated group compared with the age-matched untreated and PBS-treated groups [Figures 1F and G]. These results suggest that SHED-exos injected into SMGs increase saliva secretion and reduce lymphocytic infiltration in the SMGs of NOD mice.

SHED-exos are taken up by glandular epithelial cells

To investigate the distribution of SHED-exos, PKH-26-exos or DiR-exos were injected into the SMGs. We found that PKH-26-exos-positive signals were expressed intensively on the 1st day and appeared to be more uniformly distributed throughout the glandular tissues on the 3rd and 7th days [Figure 2A]. In addition, DiR-exos were infused into the glands. As shown in Figure 2B–D, DiR-exos were distributed around the neck and precisely in the SMG. There was no positive intensity in heart, lung, liver, spleen, kidney, pancreas, and intestine tissues. [Figure 2E]. Further observation showed that the positive signals in SMGs lasted for more than 40 days in 14-week-old mice [Figure 2F–J].

Next, we determined whether the exosomes were taken up by glandular epithelial cells. *In vitro*, PKH-26-exos were cultured with SMG-C6 cells, primary cultured acinar, and duct cells of human SMG for 24 h. As shown in Figure 2K, there were positive signals in the cytoplasm of SMG-C6 cells, human acinar cells, and duct cells, which suggest that SHED-exos can be ingested by salivary glandular epithelial cells to perform further functions.

SHED-exos upregulate the expression of the tight junction proteins ZO-1 and occludin

Fluid secretion can be accomplished through either the aquaporin 5 (AQP5)-mediated transcellular or tight junction-mediated paracellular route.[28,29] We collected labial gland tissues from SS patients and found that the expression levels of AQP5, ZO-1, occludin, and claudin-4 were significantly decreased compared with those in controls. SHED-exos incubation (200 μg/mL) with labial gland tissues from SS patients for 24 h remarkably increased the expression of ZO-1 and partially recovered the level of occludin but did not affect the contents of AQP5 and claudin-4 [Figure 3A–D]. When SMG-C6 cells were cultured with SHED-exos for 24 h, the expression of ZO-1 and occludin was increased [Figure 3E–G]. In addition, considering that the redistribution of tight junction proteins also affects their function, we further examined the location of ZO-1 and occludin. As shown in Figure 3H, SHED-exos did not change their distribution in SMG-C6 cells.

ZO-1 is required for the SHED-exo-induced increase in paracellular permeability

TER is an important indicator used to evaluate the function of tight junctions, and decreased TER is associated with increased paracellular permeability. In this study, the basal TER value of untreated SMG-C6

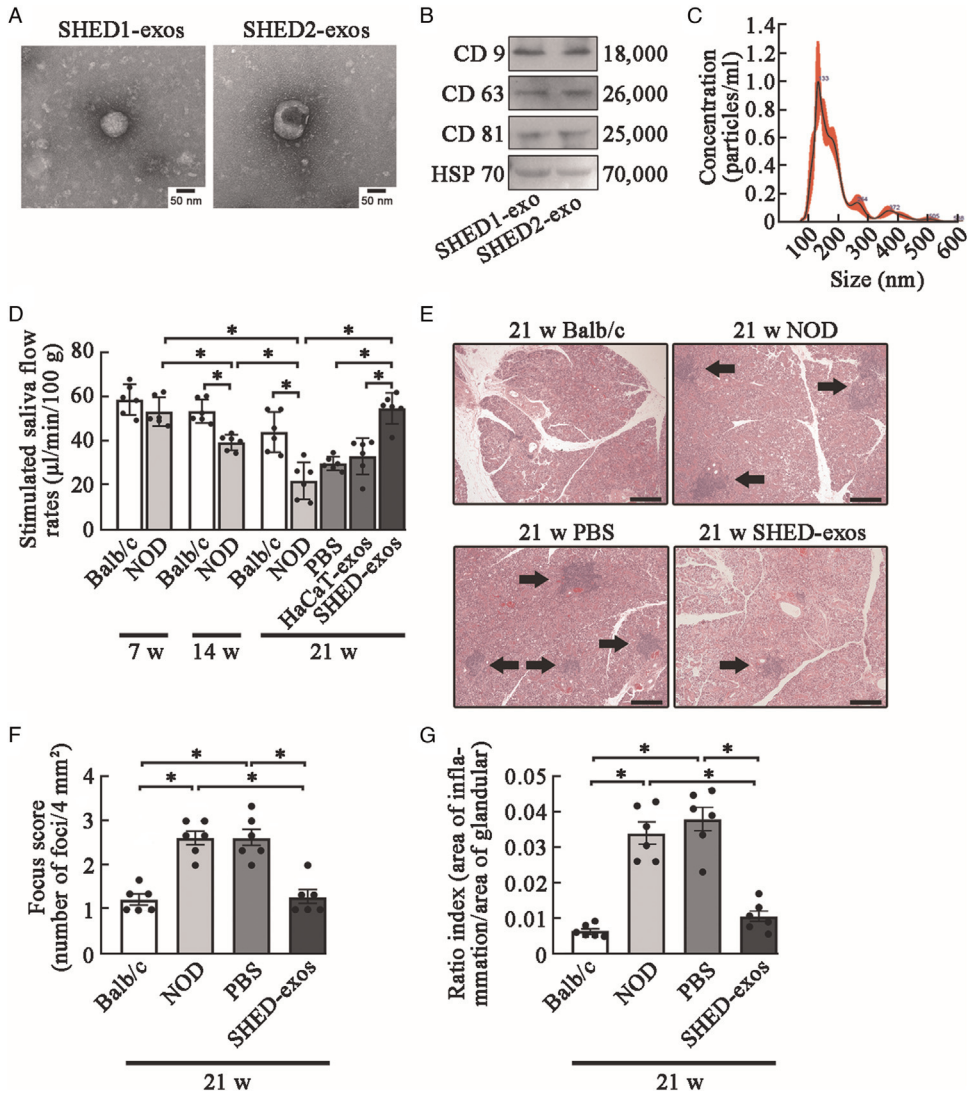

Figure 1: SHED-exos increased the saliva secretion and ameliorated lymphocytic infiltration in the SMG of NOD mice. (A) The microstructure of SHED-exos. (B) The expressions of CD9, CD63, CD81, and HSP70 in SHED-exos. (C) The size distribution and particle concentration of SHED-exos. (D) SHED-exos, HaCaT-exos, and PBS were injected into the SMGs of 14-week-old NOD mice. The stimulated saliva flow rates were measured at 21 weeks. Bars show the mean ± standard deviation ($n = 6$). (E) Representative pictures of hematoxylin-eosin staining SMGs in 21-week-old BALB/c mice and NOD mice with or without SHED-exos injection. Inflammatory cell foci are shown with arrows. Scale bar, 200 μm. (F) and (G) The degree of inflammatory infiltration in the SMGs of NOD mice was evaluated by the focus score and the ratio index. Bars show the mean ± standard error ($n = 6$). $^{*}P < 0.01$. HSP70: Heat shock protein 70; NOD: Non-obese diabetic; PBS: Phosphate buffer saline; SHED: Stem cells from human exfoliated deciduous teeth; SMG: Submandibular gland.

monolayers was 589.00 ± 23.31 Ω/cm^2, which was consistent with our previous studies.[30] SHED-exos induced a visible drop in TER values at 24 h and 48 h [Figure 3I]. These results suggest that the therapeutic effect of SHED-exos in sialadenitis may involve enhancing ZO-1 and occludin expression and improving paracellular permeability in SMGs.

ZO-1 plays crucial roles in both basal salivary epithelial barrier function and paracellular transport.[31] To confirm that the increased paracellular permeability of SHED-exos was related to ZO-1, we conducted ZO-1 depletion and rescue experiments. Compared with control cells, ZO-1 protein expression markedly reduced in ZO-1 knockout cells and recovered in ZO-1 rescue cells [Figure 3J]. Compared with the control cells, ZO-1 knockout did not affect the basic TER values, which was consistent with our previous study.[31] Furthermore, the decreased TER values induced by SHED-exos were abolished in ZO-1 knockout cells and reappeared in ZO-1 rescue cells [Figure 3K], which suggests that ZO-1 is required for the SHED-exo-induced increase in paracellular permeability.

Akt/GSK-3β pathway mediates SHED-exo-induced ZO-1 expression and increased paracellular permeability

To explore the regulatory mechanism of SHED-exos on ZO-1, we performed an miRNA microarray of SHED-exos, and 180 exosomal miRNAs were identified and profiled, as shown in Supplementary Table 3, http://links.lww.com/CM9/B445. The original data were deposited in Gene Expression Omnibus database and the accession number was GSE199497. KEGG pathway classification analysis of exosomal miRNAs target genes was performed

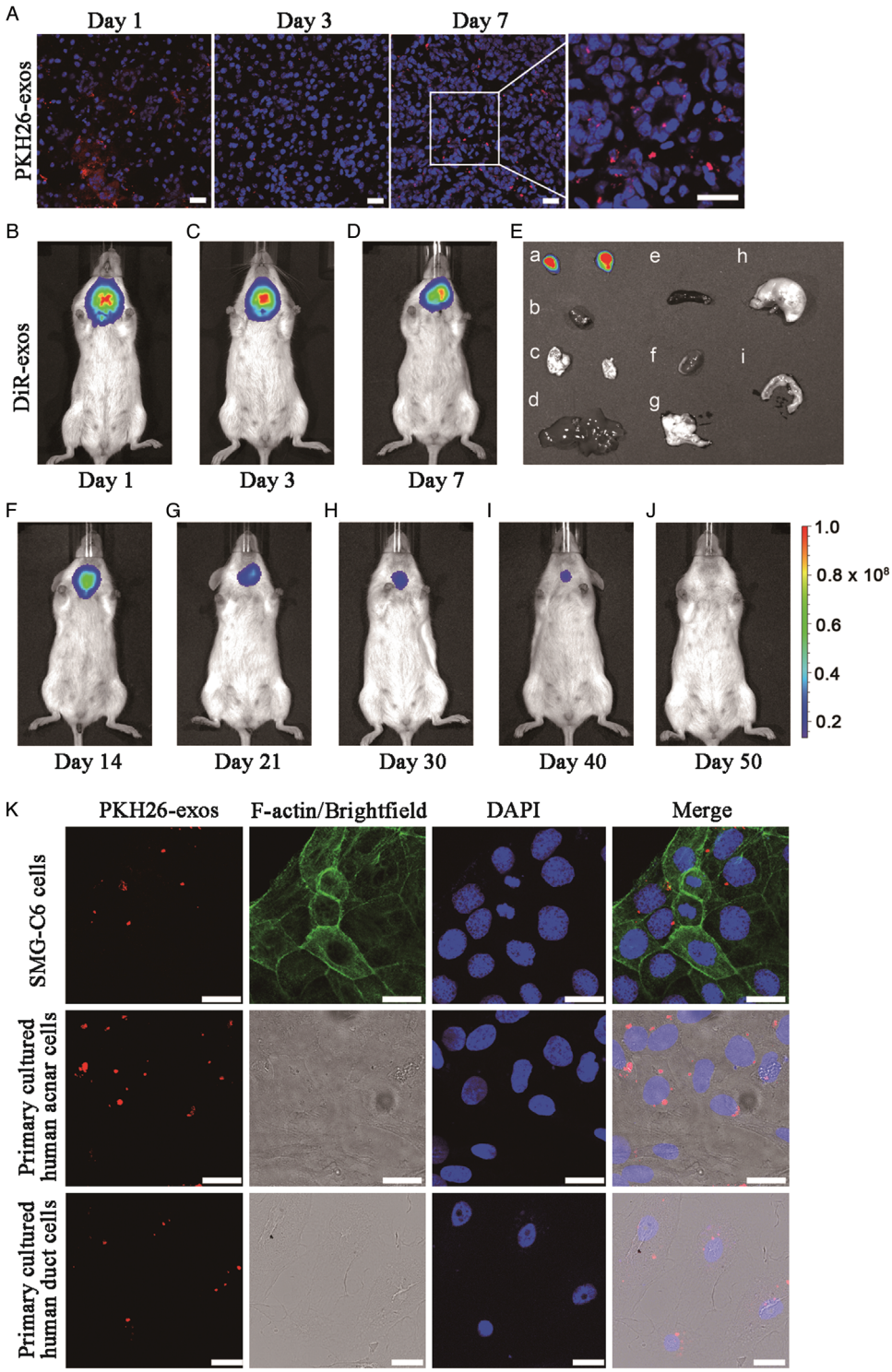

Figure 2: SHED-exos are taken up by glandular epithelial cells. (A) Representative appearances of SMGs on the 1st, 3rd, and 7th days after PKH26-exos (red) injection. Scale bar, 200 μm. Nuclei were stained with DAPI (blue). (B–D) Bioluminescence was detected on the 1st, 3rd, and 7th days after injection of DiR-exos. (E) Organs were harvested and detected on the 7th day. a: SMG; b: heart; c: lung; d: liver; e: spleen; f: kidney; g: pancreas tissue; h: stomach; i: intestines. (F–J) Bioluminescence was detected on the 14th, 21st, 30th, 40th, and 50th days after injection of DiR-exos. (K) The uptake of PKH26-exos (red) by SMG-C6 cells, primary cultured human SMG acinar, and duct cells. DAPI (blue), F-actin (green). Scale bar, 200 μm. DAPI: 4′, 6-diamidino-2-phenylindole; exos: Exosomes; SHED: Stem cells from human exfoliated deciduous teeth; SMG: Submandibular gland.

[Figure 4 left panel]. The majority of the target genes mediating signal transduction were further listed in the right panel of Figure 4, which suggested that the PI3K/Akt pathway might play an important role. Moreover, in SHED-exo-treated SMGs of NOD mice, the ratios of p-Akt/Akt and p-GSK-3β/GSK-3β were decreased, but ZO-1 was increased [Figures 5A–E]. *In vitro*, the SMGs of 14-week-old NOD mice and human SMG tissues were collected and cultured with 200 μg/mL SHED-exos for 24 h. We also found that SHED-exos decreased the levels of

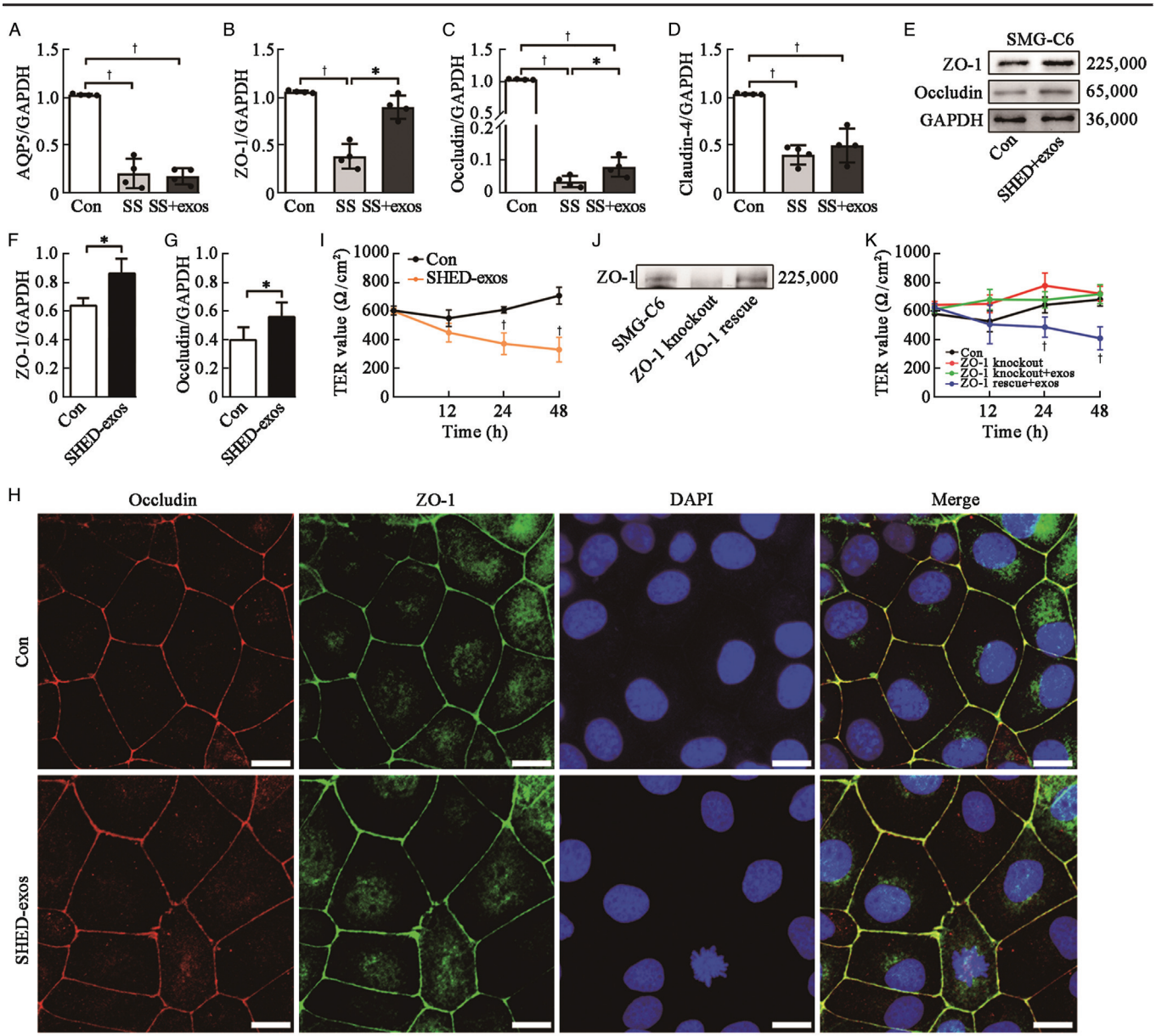

Figure 3: SHED-exos upregulate ZO-1 expressions and increased paracellular permeability in a ZO-1 dependent manner. (A–D) mRNA expressions of AQP5, ZO-1, occludin, and claudin-4 in four control glands and four SS labial glands with or without stimulation of 200 μg/mL SHED-exos for 24 h. SMG-C6 cells were cultured and collected from four independent experiments. (E) Expressions of ZO-1 and occludin in SMG-C6 cells stimulated with 200 μg/mL SHED-exos for 24 h. (F) and (G) Quantitative analysis of ZO-1 and occludin expressions normalized to GAPDH. (H) The distribution of ZO-1 and occludin were examined in SMG-C6 cells with or without SHED-exos. ZO-1 (red), occludin (green), DAPI (blue). Scale bar, 20 μm. (I) The effects of SHED-exos on TER in SMG-C6 cells. (J) ZO-1 expression in ZO-1 knockout cells and "rescued" cells. (K) The effects of SHED-exos on TER in control, ZO-1 knockout, and ZO-1 rescued SMG-C6 cells. Bars show the mean ± standard deviation ($n = 4$). $^{*}P<0.05$, $^{\dagger}P<0.01$. AQP5: Aquaporin 5; Con: Control; DAPI: 4′, 6-diamidino-2-phenylindole; Exos: Exosomes; GAPDH: Glyceraldehyde-3-phosphate dehydrogenase; mRNA: Messenger RNA; SHED: Stem cells from human exfoliated deciduous teeth; SMG: Submandibular gland; SS: Sjögren's syndrome; TER: Transepithelial electrical resistance; ZO-1: Zonula occluden-1.

p-Akt/Akt and p-GSK-3β/GSK-3β, and increased ZO-1/glyceraldehyde-3-phosphate dehydrogenase (GAPDH), compared with the untreated control [Supplementary Figure 2, http://links.lww.com/CM9/B445]. Furthermore, SHED-exos incubation for 24 h decreased the ratios of p-Akt/Akt and p-GSK-3β/GSK-3β and increased the ZO-1 levels in SMG-C6 cells. Pretreatment with insulin-like growth factor 1 (IGF1), an Akt upstream molecule PI3K agonist, abolished SHED-exo-induced responses. IGF1 alone increased p-Akt/Akt and p-GSK-3β/GSK-3β expression but decreased ZO-1 expression [Figure 5F–J]. These results suggest that Akt/GSK-3β signaling molecules negatively regulate ZO-1 expression and that SHED-exos increase ZO-1 expression via the Akt/GSK-3β pathway.

Furthermore, SHED-exos decreased the TER level, which could be attenuated by IGF1 preincubation. IGF1 treatment alone increased TER levels [Figure 5K]. To further reveal whether ZO-1 was involved in the SHED-exo-induced increase in paracellular permeability via the Akt/GSK-3β pathway, a TER assay was performed on ZO-1 knockout cells. As shown in Figure 5L, SHED-exos- or IGF1-induced changes in the TER value disappeared in ZO-1 knockout SMG-C6 cells. These results suggest that

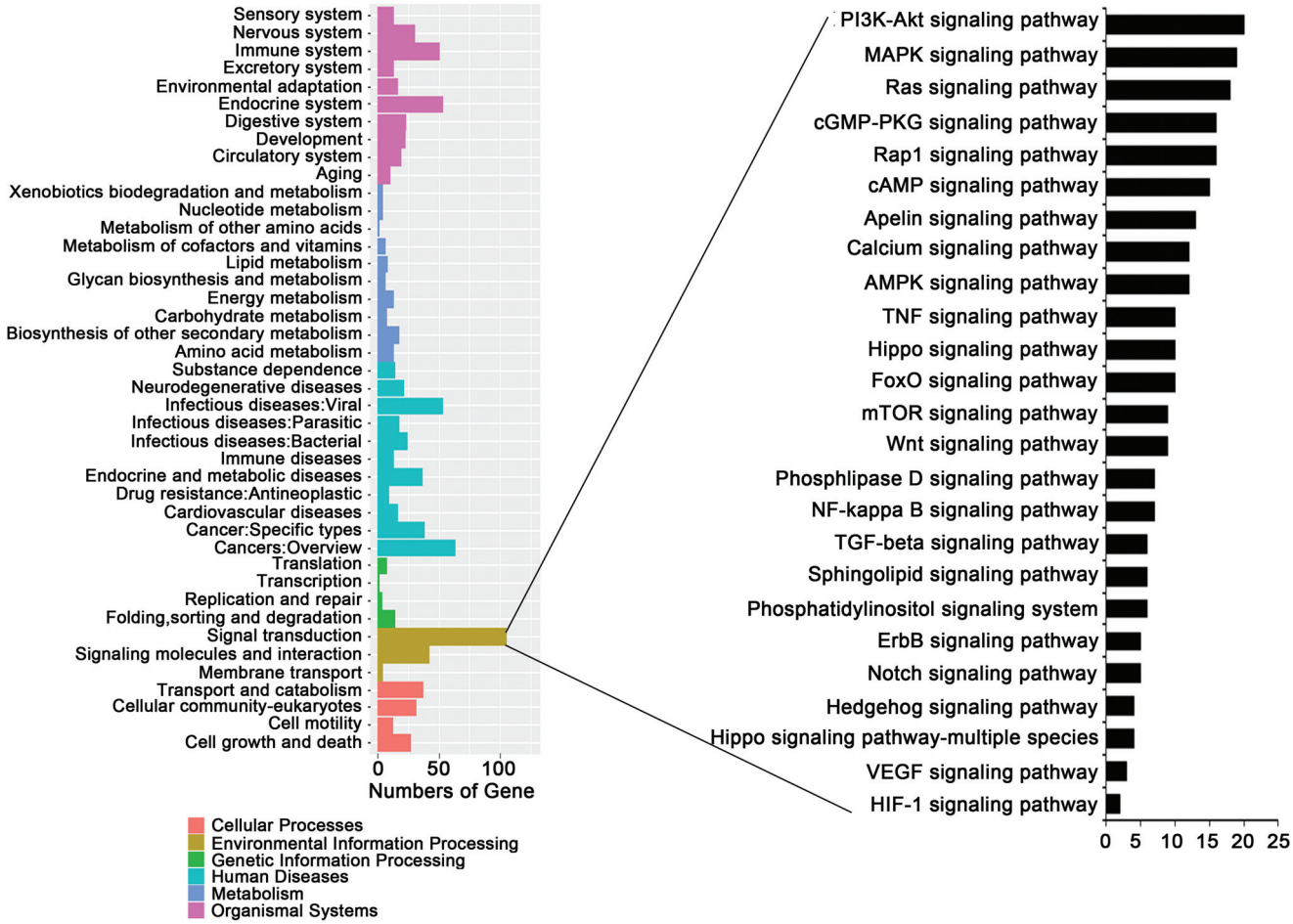

Figure 4: The Akt signaling pathway of exosamal miRNAs target genes. Left panel: Signaling pathway analysis from KEGG pathway classification of exosomal miRNAs target genes. Right panel: The majority of signal transduction mediated by target genes. miRNA: MicroRNA; KEGG: Kyoto Encyclopedia of Genes and Genomes; PI3K-Akt: Phosphatidylinositol 3 kinase (PI3K)-protein kinaseB (AKT); MAPK: Mitogen-activated protein kinase; cGMP-PKG: Cyclic guanosine monophosphate-cGMP-dependent protein kinase; Rap1: RAS-associated protein 1; camp: Cyclic Adenosine monophosphate; AMPK: Adenosine 5'-monophosphate-activated protein kinase; TNF: Tumor necrosis factor; FoxO: Forkhead Box O; mTOR: Mammalian target of rapamycin; Wnt: Wingless/Integrated; ErbB: Epidermal growth factor receptor; VEGF: Vascular endothlial growth.

the increased paracellular permeability induced by SHED-exos is related to Akt/GSK-3β pathway targeting at ZO-1.

Slug is involved in the SHED-exo-induced decrease in ZO-1

Slug, a Snail family transcription factor and the downstream signaling molecule of GSK-3β, is reported to act as a transcriptional repressor of several tight junction proteins, such as claudin-1, occludin, and ZO-1 in Madin-Darbey canine kidney (MDCK) cells and claudin-3 in SMG-C6 cells.[32,33] In the present study, SHED-exos decreased the Slug level in both NOD and human SMG tissues [Figures 5A, D and Supplementary Figure 2, http://links.lww.com/CM9/B445] and SMG-C6 cells [Figures 5M and N] but did not change Snail expression [Figures 5M–O]. Moreover, IGF1 preincubation abolished the SHED-exo-induced Slug decrease and ZO-1 increase responses. IGF1 alone increased Slug expression but downregulated ZO-1 levels [Figures 5F–J]. These results suggest that Slug acts as a transcriptional repressor of ZO-1 expression. To further reveal whether Slug binds to the ZO-1 gene directly, the promoter region of the rat ZO-1 gene was isolated and fused to the luciferase reporter vector. Transient transfection assays in the presence of pCMV6 plasmid containing Slug coding sequence (pCMV6-Slug) revealed that Slug significantly repressed wild-type ZO-1 promoter activity [Figure 5P]. These results suggest that SHED-exos suppress Slug expression by inhibiting the Akt/GSK-3β pathway, thereby decreasing the transcriptional inhibition of Slug to ZO-1 and finally enhancing ZO-1 expression.

SHED-exo intraductal infusion into the SMG restores saliva secretion in NOD mice

Stem cell-based cell therapy is commonly performed using intravenous injection or local administration. For the exocrine glands, intraductal infusion is also a good choice. To facilitate the clinical application of SHED-exos, we infused SHED-exos through the orifice of the submandibular duct in 14-week-old NOD mice and collected the SMGs at 21 weeks. As shown in Figure 6A, DiR-exo intensities were observed in the neck area on the 1st day and 14th day after infusion and even on the 49th day. As expected, the saliva flow rate was significantly increased in SHED-exo-infused mice compared with that in the PBS group

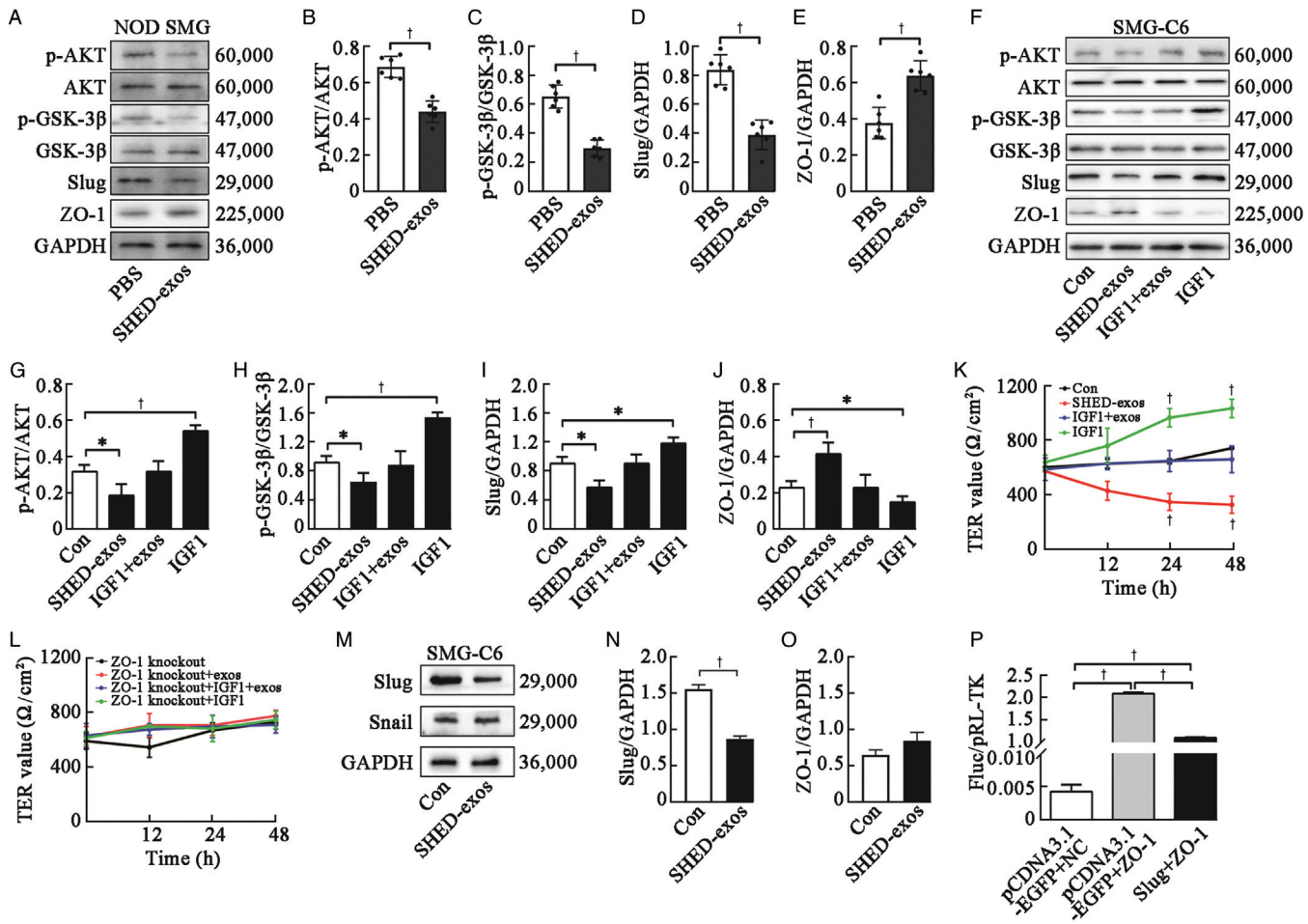

Figure 5: SHED-exos regulated ZO-1 expression via Akt/GSK-3β/Slug pathway. (A) Expressions of p-Akt, Akt, p-GSK-3β, GSK-3β, Slug, and ZO-1 in SHED-exos treated gland. (B–E) Quantitative analysis of p-Akt/Akt, p-GSK-3β/GSK-3β, Slug/GAPDH, and ZO-1/GAPDH. (F) Expressions of p-Akt, Akt, p-GSK-3β, GSK-3β, Slug, and ZO-1 in SMG-C6 cells treated with SHED-exos, pre-incubated with 100 ng/mL IGF1 for 1 h, and then SHED-exos for 24 h, and IGF1 alone. (G–J) Quantitative analysis of p-Akt/Akt, p-GSK-3β/GSK-3β, Slug/GAPDH, and ZO-1/GAPDH. (K) The effects of Akt activation by IGF1 on SHED-exos-modulated TER. (L) The effects of Akt activation by IGF1 on SHED-exos-modulated TER in ZO-1 knockout cells. (M–O) The Slug and Snail expressions in SHED-exos treated cells. (P) Slug bound to ZO-1 promoter and suppressing ZO-1 transcription. Bars show the mean ± standard deviation ($n = 6$). $^{*}P < 0.05$, $^{\dagger}P < 0.01$. GAPDH: Glyceraldehyde-3-phosphate dehydrogenase; IGF1: Insulin-like growth factor 1; NOD: Non-obese diabetic; SHED: Stem cells from human exfoliated deciduous teeth; SMG: Submandibular gland; TER: Transepithelial electrical resistance; ZO-1: Zonula occluden-1; Con: Control; Fluc: Firefly luciferase; p-Akt: Phospho-protein kinase B; p-GSK-3β: Phospho-glycogen synthase kinase 3β; Exos: Exosomes.

[Figure 6B]. After treatment, inflammatory cell infiltration in the SMG was alleviated. The focus scores and ratio index were decreased in the glands infused with SHED-exos compared with those in the PBS group [Figure 6C–E]. Moreover, p-Akt/Akt, p-GSK-3β/GSK-3β, and Slug expression was decreased, and ZO-1 was increased in SHED-exo-infused glands compared with PBS controls [Figure 6F–J].

Discussion

In the present study, we demonstrated that local application of SHED-exos exhibited therapeutic benefits for sialadenitis induced by NOD. SHED-exos injected or infused into SMGs of NOD mice increased the saliva flow rate and alleviated glandular inflammation. Furthermore, SHED-exos improved paracellular permeability by elevating ZO-1 expression. A mechanistic study showed that inhibition of the Akt/GSK-3β pathway and a decrease in the transcriptional inhibition of Slug to ZO-1 were involved in promoting the secretion effect of SHED-exos [Figure 6K].

Recently, exosomes obtained from labial gland-derived stem cells were demonstrated to promote the proliferation of regulatory T (Treg) cells, inhibit T helper cell 17 (Th17) cells, ameliorate inflammatory infiltration in the exocrine glands and restore salivary gland secretory function in mouse models of SS.[34] SHEDs originate from the embryonic neural crest as MSCs and are isolated from human deciduous teeth.[35] Based on the high proliferative capacity, and low immunogenicity and teratogenicity, SHEDs are safer and more convenient mediators, compared to other MSCs.[36,37] In our previous study, intravenous injection of SHEDs exerted a protective effect on saliva secretion in the early phase of NOD mice by regulating T cell differentiation and improving the inflammatory microenvironment.[12] Here, we demonstrate that local injection of SHED-exos into the SMGs of 14-week-old NOD mice, a clinical phase of SS, significantly promotes salivary secretion and decreases lymphocytic infiltration in the SMGs of NOD mice. Moreover, we demonstrated that intraductal infusion of SHED-exos into acinar units was an effective therapy for

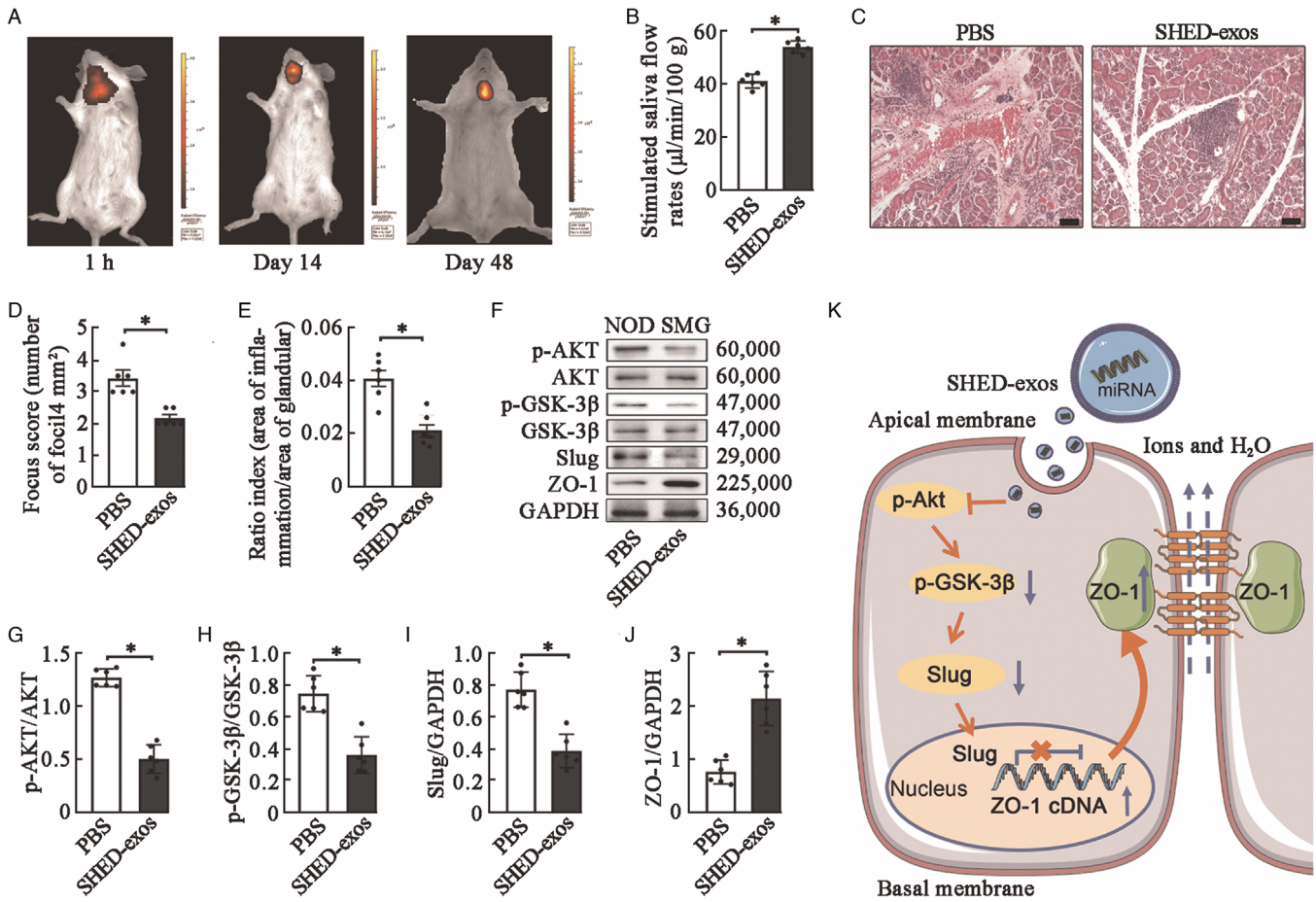

Figure 6: Intraductal infusion with SHED-exos. (A) Bioluminescence was detected on the 1st, 14th, and 49th days after intraductal injection of DiR-exos. (B) The stimulated saliva flow rates were measured and analyzed at 21 weeks. (C) Representative pictures of hematoxylin-eosin staining of SMGs in 21-week-old NOD mice with or without SHED-exos treatment. Scale bar, 200 μm. (D) and (E) The degree of inflammatory infiltration in the SMG of NOD mice was evaluated by the focus score and the ratio index. Bars show the mean ± standard error ($n = 6$). (F) Expressions of p-Akt, Akt, p-GSK-3β, GSK-3β, Slug, and ZO-1 in SHED-exos treated gland. (G–J) Quantitative analysis of p-Akt normalized to Akt, p-GSK-3β normalized to GSK-3β, and Slug and ZO-1 normalized to GAPDH. Bars show the mean ± standard deviation ($n = 6$). (K) Schematic illustration showing that the mechanism of SHED-exos increased paracellular permeability of salivary gland cells via Akt/GSK-3β/Slug-mediated ZO-1 expression. $^{*}P < 0.01$. GAPDH: Glyceraldehyde-3-phosphate dehydrogenase; NOD: Non-obese diabetic; SHED: Stem cells from human exfoliated deciduous teeth; SMG: Submandibular gland; ZO-1: Zonula occluden-1; PBS: Phosphate buffer saline; Exos: Exosomes; Akt: Protein kinase B; GSK: Glycogen synthase kinase; miRNA: MicroRNA.

sialadenitis induced by NOD, which may provide a new feasible strategy to reduce the invasiveness of percutaneous needle injection and improve delivery to permeate the entire gland parenchyma. SHED-exos administered by local application could be taken up by salivary epithelial cells and the positive signals lasted for more than 40 days.

Glandular epithelial cells are responsible for saliva secretion. Gland epithelial cells are the primary target of immune attack in SS, resulting in impaired expression, location, and function of secretion-related molecules, such as AQP5 and tight junction proteins.[38,39] Tight junctions are protein complexes related to cell–cell interactions and play an essential role in regulating water and solute transport through the paracellular pathway in salivary glands.[40,41] A previous study indicated that disruption of tight junction integrity and downregulation of ZO-1 and occludin were observed in minor salivary glands from SS patients.[42] Our previous study also showed that the elevated IL-17 in the SMGs of NOD mice impaired the expression of ZO-1, claudin-4, and their apicolateral membrane distribution through the nuclear factor kappa-B (NF-κB) signaling pathway, which might contribute to salivary gland dysfunction in SS.[43] In the present study, ZO-1, occludin, and claudin-4 expression was decreased in the labial glands of SS patients, which indicated that the disruption in tight junction integrity was involved in decreased saliva secretion in SS. Local injection or perfusion of SHED-exos significantly increased ZO-1 expression in the salivary glands of NOD mice.

ZO-1 is an important intracellular scaffold tight junction (TJ) protein that links the transmembrane TJ proteins with actin cytoskeleton.[28] Decreased expression of ZO-1 results in impaired intestinal tight junction barrier and increased intestinal paracellular permeability.[44] Knockdown of ZO-1 in HK-2 cells by ZO-1 small interfering RNA increased the permeability to fluorescein isothiocyanate (FITC)-detran.[45] Increasing ZO-1 expression protects against hypoxia/reperfusion-induced brain vascular endothelial permeability.[46] ZO-1 knockdown increased permeability of the retinal pigment epithelium.[47] However, other studies have showed that ZO-1 knockdown exhibits a higher paracellular flux rate in

MDCK cells.[48] Knockdown of ZO-1 in HeLa cells inhibited normal trafficking and cell–cell communication.[49] These results suggest that the effect of ZO-1 on paracellular permeability may vary depending on the cell type. In rabbit SMGs, ZO-1 plays a critical role in the saliva secretion, particularly in maintaining TJ integrity, and the decrease or lack of ZO-1 combined with other TJ components reduced paracellular transport and led to hyposecretion.[50] TER reflects the ions that pass through claudin-based charge-selective pores (~4 Å in radius) with instantaneous (typically in seconds) high permeability.[51] Knockout of ZO-1 did not change the base TER values, which was consistent with our previous study,[31] confirming that ZO-1 alone did not obviously influence ionic permeability in normal salivary epithelium. However, SHED-exos incubation decreased TER values in SMG-C6 cells. These effects were abolished in ZO-1 knockout cells and recovered in ZO-1 rescued cells. These results indicate that SHED-exos increase the paracellular permeability of salivary gland epithelial cells via ZO-1, consequently enhancing gland secretory function.

Next, we focused on the regulatory mechanism of SHED-exos on ZO-1 expression. Based on the data from the exosomal miRNAs and KEGG analysis, we hypothesized that the PI3K-Akt pathway might contribute to the biological effect of SHED-exos. LY294002, a PI3K inhibitor, decreased B-lymphocyte viability in the labial glands of SS, which was deemed a future therapeutic option in SS.[52] Moreover, GSK-3 inhibitor-loaded osteotropic pluronic hydrogel was reported to reduce the chronic inflammatory state and the periodontal tissue damage associated with periodontitis.[53] The above studies suggest that the PI3K/Akt/GSK-3 pathway might be involved in regulating saliva secretion.

It has been shown that activation of PI3K/Akt pathway increased ZO-1, occludin, and claudin-1 expression, maintaining the normal barrier function of intestinal epithelial cells.[54] In contrast, in cerebrovascular endothelial cells, activating the PI3K/Akt pathway decreased ZO-1 expression and function, destroyed the normal blood–brain barrier, and participated in the occurrence of ischemic stroke.[55] In this study, the ratios of p-Akt/Akt and p-GSK-3β/GSK-3β were decreased in SHED-exo-treated salivary glands and SMG-C6 cells, accompanied by increased ZO-1 expression and paracellular permeability. *In vitro*, activation of the Akt pathway by IGF1 decreased ZO-1 expression and paracellular permeability. IGF1 pretreatment also depressed the increased ZO-1 expression and paracellular permeability induced by SHED-exos. More importantly, the decreased paracellular permeability induced by IGF1 disappeared in ZO-1 knockout cells. These results suggest that the Akt/GSK-3β pathway negatively regulates ZO-1 expression. SHED-exos increase paracellular permeability by inhibiting Akt/GSK-3β pathway-mediated ZO-1 expression.

Slug, one of the Snail family proteins, is a key inducer of the epithelial-mesenchymal transition through mediating the transcriptional repression of tight junctions, adherens junctions, and desmosomes.[56] Our previous study showed that Slug activated by tumor necrosis factor-α can bind to claudin-3, thereby destroying the normal barrier function of epithelial cells in SMGs.[32] However, whether Slug can bind to ZO-1 and participate in saliva secretion is unknown. In this study, SHED-exos decreased Slug expression *in vivo* and *in vitro*, and the results from a double luciferase reporter gene assay directly confirmed that Slug could bind to the ZO-1 promotor and repress its activity. Activation of Akt can phosphorylate GSK-3β and inhibit GSK-3β activity, thereby preventing the degradation of Slug, resulting in decreased expression of ZO-1, occludin, and E-cadherin in a study of renal function injury caused by ketamine.[57] In the present study, SHED-exos decreased the activation of the Akt/GSK-3β pathway. Dephosphorylation of GSK-3β might promote Slug degradation, thereby decreasing transcription inhibition of ZO-1. Next, more studies are needed to explore which SHED-exos miRNAs are involved in regulating the Akt/GSK-3β/Slug signaling pathway.

In summary, we demonstrated that ZO-1 is a crucial target in mediating SHED-exo-modulated paracellular transport in the submandibular epithelium. SHED-exos increased ZO-1 expression and paracellular permeability of salivary cells by inhibiting the Akt/GSK-3/Slug pathway. Local application of SHED-exos significantly decreased SMG injury induced by SS. These findings enrich our understanding of the mechanism involved in SHED-exo-modulated saliva secretion and provide a potential therapeutic strategy for the local application of SHED-exos to sialadenitis induced by SS.

Acknowledgment

We thank Dr. David O. Quissell from School of Dentistry, University of Colorado Health Sciences Center, Denver, CO, USA, for the generous gift of rat SMG-C6 cell line.

Funding

This work was supported by grants from the National Natural Science Foundation of China (Nos. 81974151 and 81771088) and Peking University-Tason Stomatology Development Fund.

Conflicts of interest

None.

References

1. Nocturne G, Mariette X. Sjögren syndrome-associated lymphomas: an update on pathogenesis and management. Br J Haematol 2015;168:317–327. doi: 10.1111/bjh.13192.
2. Brito-Zerón P, Acar-Denizli N, Zeher M, Rasmussen A, Seror R, Theander E, *et al*. Influence of geolocation and ethnicity on the phenotypic expression of primary Sjögren's syndrome at diagnosis in 8310 patients: a cross-sectional study from the big data Sjögren project consortium. Ann Rheum Dis 2017;76:1042–1050. doi: 10.1136/annrheumdis-2016-209952.
3. Haldorsen K, Moen K, Jacobsen H, Jonsson R, Brun JG. Exocrine function in primary Sjögren syndrome: natural course and prognostic factors. Ann Rheum Dis 2008;67:949–954. doi: 10.1136/ard.2007.074203.

4. Anaya JM, Restrepo-Jiménez P, Rodríguez Y, Rodríguez-Jiménez M, Acosta-Ampudia Y, Monsalve DM, *et al*. Sjögren's syndrome and autoimmune thyroid disease: two sides of the same coin. Clin Rev Allergy Immunol 2019;56:362–374. doi: 10.1007/s12016-018-8709-9.
5. Xuan L, Zhang YD, Li L, Zeng YP, Zhang HZ, Wang J, *et al*. Clinical profile and significance of mucocutaneous lesions of primary Sjögren's syndrome: a large cross-sectional study with 874 patients. Chin Med J 2017;130:2423–2428. doi: 10.4103/0366-6999.216403.
6. Ramos-Casals M, Tzioufas AG, Stone JH, Sisó A, Bosch X. Treatment of primary Sjögren syndrome: a systematic review. JAMA 2010;304:452–460. doi: 10.1001/jama.2010.1014.
7. Mariette X, Criswell LA. Primary Sjögren's syndrome. N Engl J Med 2018;378:931–939. doi: 10.1056/NEJMcp1702514.
8. Li H, Liu Z, Gong Y, Jiang Z, Zhang Y, Dai Y, *et al*. Application of immunosuppressant facilitates the therapy of optic neuritis combined with Sjögren's syndrome. Chin Med J 2014;127:3098–3104. doi: 10.3760/cma.j.issn.0366-6999.20133253.
9. Wong SK, Chin KY, Suhaimi FH, Fairus A, Ima-Nirwana S. Animal models of metabolic syndrome: a review. Nutr Metab (Lond) 2016;13:65. doi: 10.1186/s12986-016-0123-9.
10. Xu J, Wang D, Liu D, Fan Z, Zhang H, Liu O, *et al*. Allogeneic mesenchymal stem cell treatment alleviates experimental and clinical Sjögren syndrome. Blood 2012;120:3142–3151. doi: 10.1182/blood-2011-11-391144.
11. Matsumura-Kawashima M, Ogata K, Moriyama M, Murakami Y, Kawado T, Nakamura S. Secreted factors from dental pulp stem cells improve Sjögren's syndrome via regulatory T cell-mediated immunosuppression. Stem Cell Res Ther 2021;12:182. doi: 10.1186/s13287-021-02236-6.
12. Du ZH, Ding C, Zhang Q, Zhang Y, Ge XY, Li SL, *et al*. Stem cells from exfoliated deciduous teeth alleviate hyposalivation caused by Sjögren syndrome. Oral Dis 2019;25:1530–1544. doi: 10.1111/odi.13113.
13. Kinnaird T, Stabile E, Burnett MS, Shou M, Lee CW, Barr S, *et al*. Local delivery of marrow-derived stromal cells augments collateral perfusion through paracrine mechanisms. Circulation 2004;109:1543–1549. doi: 10.1161/01.CIR.0000124062.31102.57.
14. Ogata K, Katagiri W, Osugi M, Kawai T, Sugimura Y, Hibi H, *et al*. Evaluation of the therapeutic effects of conditioned media from mesenchymal stem cells in a rat bisphosphonate-related osteonecrosis of the jaw-like model. Bone 2015;74:95–105. doi: 10.1016/j.bone.2015.01.011.
15. Sugimura-Wakayama Y, Katagiri W, Osugi M, Kawai T, Ogata K, Sakaguchi K, *et al*. Peripheral nerve regeneration by secretomes of stem cells from human exfoliated deciduous teeth. Stem Cells Dev 2015;24:2687–2699. doi: 10.1089/scd.2015.0104.
16. Ogata K, Katagiri W, Hibi H. Secretomes from mesenchymal stem cells participate in the regulation of osteoclastogenesis in vitro. Clin Oral Investig 2017;21:1979–1988. doi: 10.1007/s00784-016-1986-x.
17. Kowal J, Arras G, Colombo M, Jouve M, Morath JP, Primdal-Bengtson B, *et al*. Proteomic comparison defines novel markers to characterize heterogeneous populations of extracellular vesicle subtypes. Proc Natl Acad Sci U S A 2016;113:E968–E977. doi: 10.1073/pnas.1521230113.
18. van Niel G, Charrin S, Simoes S, Romao M, Rochin L, Saftig P, *et al*. The tetraspanin CD63 regulates ESCRT-independent and -dependent endosomal sorting during melanogenesis. Dev Cell 2011;21:708–721. doi: 10.1016/j.devcel.2011.08.019.
19. Riazifar M, Mohammadi MR, Pone EJ, Yeri A, Lässer C, Segaliny AI, *et al*. Stem cell-derived exosomes as nanotherapeutics for autoimmune and neurodegenerative disorders. ACS Nano 2019;13:6670–6688. doi: 10.1021/acsnano.9b01004.
20. Whiteside TL. Exosome and mesenchymal stem cell cross-talk in the tumor microenvironment. Semi Immunol 2018;35:69–79. doi: 10.1016/j.smim.2017.12.003.
21. Doeppner TR, Herz J, Görgens A, Schlechter J, Ludwig AK, Radtke S, *et al*. Extracellular vesicles improve post-stroke neuroregeneration and prevent postischemic immunosuppression. Stem Cells Transl Med 2015;4:1131–1143. doi: 10.5966/sctm.2015-0078.
22. Almazroa A, Sun W, Alodhayb S, Raahemifar K, Lakshminarayanan V. Optic disc segmentation for glaucoma screening system using fundus images. Clin Ophthalmol 2017;11:2017–2029. doi: 10.2147/OPTH.S140061.
23. Lonati C, Bassani GA, Brambilla D, Leonardi P, Carlin A, Maggioni M, *et al*. Mesenchymal stem cell-derived extracellular vesicles improve the molecular phenotype of isolated rat lungs during ischemia/reperfusion injury. J Heart Lung Transplant 2019;38:1306–1316. doi: 10.1016/j.healun.2019.08.016.
24. Miura M, Gronthos S, Zhao M, Lu B, Fisher LW, Robey PG, *et al*. SHED: stem cells from human exfoliated deciduous teeth. Proc Natl Acad Sci U S A 2003;100:5807–5812. doi: 10.1073/pnas.0937635100.
25. Ding C, Cong X, Zhang Y, Yang NY, Li SL, Wu LL, *et al*. Hypersensitive mAChRs are involved in the epiphora of transplanted glands. J Dent Res 2014;93:306–312. doi: 10.1177/0022034513519107.
26. Quissell DO, Barzen KA, Gruenert DC, Redman RS, Camden JM, Turner JT. Development and characterization of SV40 immortalized rat submandibular acinar cell lines. In Vitro Cell Dev Biol Anim 1997;33:164–173. doi: 10.1007/s11626-997-0137-8.
27. Yang WW, Yang LQ, Zhao F, Chen CW, Xu LH, Fu J, *et al*. Epiregulin promotes lung metastasis of salivary adenoid cystic carcinoma. Theranostics 2017;7:3700–3714. doi: 10.7150/thno.19712.
28. Tsukita S, Furuse M, Itoh M. Multifunctional strands in tight junctions. Nat Rev Mol Cell Biol 2001;2:285–293. doi: 10.1038/35067088.
29. Mitic LL, Anderson JM. Molecular architecture of tight junctions. Annu Rev Physiol 1998;60:121–142. doi: 10.1146/annurev.physiol.60.1.121.
30. Ding C, Li L, Su YC, Xiang RL, Cong X, Yu HK, *et al*. Adiponectin increases secretion of rat submandibular gland via adiponectin receptors-mediated AMPK signaling. PLoS One 2013;8:e63878. doi: 10.1371/journal.pone.0063878.
31. Li J, Cong X, Zhang Y, Xiang RL, Mei M, Yang NY, *et al*. ZO-1 and -2 are required for TRPV1-modulated paracellular permeability. J Dent Res 2015;94:1748–1756. doi: 10.1177/0022034515609268.
32. Mei M, Xiang RL, Cong X, Zhang Y, Li J, Yi X, *et al*. Claudin-3 is required for modulation of paracellular permeability by TNF-alpha through ERK1/2/slug signaling axis in submandibular gland. Cell Signal 2015;27:1915–1927. doi: 10.1016/j.cellsig.2015.07.002.
33. Ohkubo T, Ozawa M. The transcription factor Snail downregulates the tight junction components independently of E-cadherin downregulation. J Cell Sci 2004;117:1675–1685. doi: 10.1242/jcs.01004.
34. Li B, Xing Y, Gan Y, He J, Hua H. Labial gland-derived mesenchymal stem cells and their exosomes ameliorate murine Sjögren's syndrome by modulating the balance of Treg and Th17 cells. Stem Cell Res Ther 2021;12:478. doi: 10.1186/s13287-021-02541-0.
35. Ko CS, Chen JH, Su WT. Stem cells from human exfoliated deciduous teeth: a concise review. Curr Stem Cell Res Ther 2020;15:61–76. doi: 10.2174/1574888X14666191018122109.
36. Kunimatsu R, Nakajima K, Awada T, Tsuka Y, Abe T, Ando K, *et al*. Comparative characterization of stem cells from human exfoliated deciduous teeth, dental pulp, and bone marrow-derived mesenchymal stem cells. Biochem Biophys Res Commun 2018;501:193–198. doi: 10.1016/j.bbrc.2018.04.213.
37. Isobe Y, Koyama N, Nakao K, Osawa K, Ikeno M, Yamanaka S, *et al*. Comparison of human mesenchymal stem cells derived from bone marrow, synovial fluid, adult dental pulp, and exfoliated deciduous tooth pulp. Int J Oral Maxillofac Surg 2016;45:124–131. doi: 10.1016/j.ijom.2015.06.022.
38. Tsunawaki S, Nakamura S, Ohyama Y, Sasaki M, Ikebe-Hiroki A, Hiraki A, *et al*. Possible function of salivary gland epithelial cells as nonprofessional antigen-presenting cells in the development of Sjögren's syndrome. J Rheumatol 2002;29:1884–1896.
39. Mitsias DI, Kapsogeorgou EK, Moutsopoulos HM. The role of epithelial cells in the initiation and perpetuation of autoimmune lesions: lessons from Sjögren's syndrome (autoimmune epithelitis). Lupus 2006;15:255–261. doi: 10.1191/0961203306lu2290rr.
40. Anderson JM. Molecular structure of tight junctions and their role in epithelial transport. News Physiol Sci 2001;16:126–130. doi: 10.1152/physiologyonline.2001.16.3.126.
41. Miyoshi J, Takai Y. Structural and functional associations of apical junctions with cytoskeleton. Biochim Biophys Acta 2008;1778:670–691. doi: 10.1016/j.bbamem.2007.12.014.
42. Ewert P, Aguilera S, Alliende C, Kwon YJ, Albornoz A, Molina C, *et al*. Disruption of tight junction structure in salivary glands from Sjögren's syndrome patients is linked to proinflammatory cytokine exposure. Arthritis Rheum 2010;62:1280–1289. doi: 10.1002/art.27362.

43. Zhang LW, Cong X, Zhang Y, Wei T, Su YC, Serrão AC, *et al*. Interleukin-17 impairs salivary tight junction integrity in Sjögren's syndrome. J Dent Res 2016;95:784–792. doi: 10.1177/0022034516634647.
44. Feng Y, Huang Y, Wang Y, Wang P, Song H, Wang F. Antibiotics induced intestinal tight junction barrier dysfunction is associated with microbiota dysbiosis, activated NLRP3 inflammasome and autophagy. PLoS One 2019;14:e0218384. doi: 10.1371/journal.pone.0218384.
45. Kim S, Kim GH. Roles of claudin-2, ZO-1 and occludin in leaky HK-2 cells. PLoS One 2017;12:e0189221. doi: 10.1371/journal.pone.0189221.
46. Li C, Zhang Y, Liu R, Mai Y. Anagliptin protected against hypoxia/reperfusion-induced brain vascular endothelial permeability by increasing ZO-1. ACS Omega 2021;6:7771–7777. doi: 10.1021/acsomega.1c00242.
47. Bao H, Yang S, Li H, Yao H, Zhang Y, Zhang J, *et al*. The interplay between E-cadherin, Connexin 43, and zona occludens 1 in retinal pigment epithelial cells. Invest Ophthalmol Vis Sci 2019;60:5104–5111. doi: 10.1167/iovs.19-27768.
48. Bilal S, Jaggi S, Janosevic D, Shah N, Teymour S, Voronina A, *et al*. ZO-1 protein is required for hydrogen peroxide to increase MDCK cell paracellular permeability in an ERK 1/2-dependent manner. Am J Physiol Cell Physiol 2018;315:C422–C431. doi: 10.1152/ajpcell.00185.2017.
49. Chai Z, Goodenough DA, Paul DL. Cx50 requires an intact PDZ-binding motif and ZO-1 for the formation of functional intercellular channels. Mol Biol Cell 2011;22:4503–4512. doi: 10.1091/mbc.E11-05-0438.
50. Cong X, Zhang Y, Shi L, Yang NY, Ding C, Li J, *et al*. Activation of transient receptor potential vanilloid subtype 1 increases expression and permeability of tight junction in normal and hyposecretory submandibular gland. Lab Invest 2012;92:753–768. doi: 10.1038/labinvest.2012.12.
51. Srinivasan B, Kolli AR, Esch MB, Abaci HE, Shuler ML, Hickman JJ. TEER measurement techniques for in vitro barrier model systems. J Lab Autom 2015;20:107–126. doi: 10.1177/2211068214561025.
52. Rivière E, Pascaud J, Tchitchek N, Boudaoud S, Paoletti A, Ly B, *et al*. Salivary gland epithelial cells from patients with Sjögren's syndrome induce B-lymphocyte survival and activation. Ann Rheum Dis 2020;79:1468–1477. doi: 10.1136/annrheumdis-2019-216588.
53. Almoshari Y, Ren R, Zhang H, Jia Z, Wei X, Chen N, *et al*. GSK3 inhibitor-loaded osteotropic Pluronic hydrogel effectively mitigates periodontal tissue damage associated with experimental periodontitis. Biomaterials 2020;261:120293. doi: 10.1016/j.biomaterials.2020.120293.
54. Zhuang Y, Wu H, Wang X, He J, He S, Yin Y. Resveratrol attenuates oxidative stress-induced intestinal barrier injury through PI3K/Akt-mediated Nrf2 signaling pathway. Oxid Med Cell Longev 2019;2019:7591840. doi: 10.1155/2019/7591840.
55. Lv Y, Liu W, Ruan Z, Xu Z, Fu L. Myosin IIA regulated tight junction in oxygen glucose-deprived brain endothelial cells via activation of TLR4/PI3K/Akt/JNK1/2/14-3-3epsilon/NF-kappaB/MMP9 signal transduction pathway. Cell Mol Neurobiol 2019;39:301–319. doi: 10.1007/s10571-019-00654-y.
56. Barrallo-Gimeno A, Nieto MA. The Snail genes as inducers of cell movement and survival: implications in development and cancer. Development 2005;132:3151–3161. doi: 10.1242/dev.01907.
57. Lin Y, Zhang C, Xiang P, Shen J, Sun W, Yu H. Exosomes derived from HeLa cells break down vascular integrity by triggering endoplasmic reticulum stress in endothelial cells. J Extracell Vesicle 2020;9:1722385. doi: 10.1080/20013078.2020.1722385.

How to cite this article: Du Z, Wei P, Jiang N, Wu L, Ding C, Yu G. SHED-derived exosomes ameliorate hyposalivation caused by Sjögren's syndrome via Akt/GSK-3β/Slug-mediated ZO-1 expression. Chin Med J 2023;136:2596–2608. doi: 10.1097/CM9.0000000000002610